Atmosphere **2015**, *6*, 650-676; doi:10.3390/atmos6050650

OPEN ACCESS

atmosphere

ISSN 2073-4433

www.mdpi.com/journal/atmosphere

Article

The Concentrations and Reduction of Airborne Particulate Matter (PM_{10}, $PM_{2.5}$, PM_1) at Shelterbelt Site in Beijing

Jungang Chen [1], Xinxiao Yu [1], Fenbing Sun [1], Xiaoxiu Lun [2], Yanlin Fu [3], Guodong Jia [1], Zhengming Zhang [4], Xuhui Liu [1], Li Mo [1] and Huaxing Bi [1,*]

[1] College of Soil and Water Conservation, Beijing Forestry University, Haidian District, 100083 Beijing, China; E-Mails: chenjungang115@163.com (J.C.); yuxinxiao345@126.com (X.Y.); sfb304@163.com (F.S.); jgd3@163.com (G.J.); liuxuhuibjfu@126.com (X.L.); moli.7@163.com (L.M.)

[2] College of Environmental Engineering, Beijing Forestry University, Haidian District, 100083 Beijing, China; E-Mail: lunxiaoxiu@bjfu.com

[3] College of Forestry, Beijing Forestry University, Haidian District, 100083 Beijing, China; E-Mail: fyl814@163.com

[4] College of Nature Conservation, Beijing Forestry University, Haidian District, 100083 Beijing, China; E-Mail: mingzhzh010@126.com

* Author to whom correspondence should be addressed; E-Mail: bhx@bjfu.edu.cn; Tel.: +86-10-6233-6756.

Academic Editor: Daniele Contini

Received: 17 January 2015 / Accepted: 22 April 2015 / Published: 18 May 2015

Abstract: Particulate matter is a serious source of air pollution in urban areas, where it exerts adverse effects on human health. This article focuses on the study of subduction of shelterbelts for atmospheric particulates. The results suggest that (1) the PM mass concentration is higher in the morning or both morning and noon inside the shelterbelts and lower mass concentrations at other times; (2) the particle mass concentration inside shelterbelt is higher than outside; (3) the particle interception efficiency of the two forest belts over the three months in descending order was PM10 > PM1 > PM2.5; and (4) the two shelterbelts captured air pollutants at rates of 1496.285 and 909.075 kg/month and the major atmospheric pollutant in Beijing city is PM10. Future research directions are to study PM mass concentration variation of shelterbelt with different tree species and different configuration.

Keywords: particulates; shelterbelt; mass concentration; meteorological factors

1. Introduction

Since China's reform and opening up, the Chinese economy has experienced rapid development for more than 30 years; however, rapid urbanization has led to increasingly complex environmental pollution problems. The government has taken intensive efforts to solve these problems by approaches such as the development of public transport, improvement in gasoline quality standards, vigorous promotion of clean production, and acceleration of the adjustment of energy structure. The use of vegetation for removing atmospheric pollutants has attracted increasing attention among scientists and urban planners [1–9]. Urban forests play an important role in reducing atmospheric pollution and improving the quality of the urban environment. Forest vegetation can capture aerosols, particulates, and other pollutants more efficiently and are characterized by higher dry deposition than other land surfaces [10–12].

Removing particles from the atmosphere to the surface of the earth is a combination of processes including five steps: (1) sedimentation; (2) diffusion; (3) turbulence; (4) washout; and (5) wet deposition [13]. The dry deposition of particles and gases is by the first three of the processes listed above. Dry deposition also described combined removal process of particulates from the atmosphere by gravity, Brownian motion, impaction, and direct interception [14]. Sedimentation occurs by agglomeration among fine particles, owing to their attractive and reactive properties. Brownian motion was the main way of moving gases and fine particulates and this movement is important for inducing fine particles to dissolve on the wet leaf surface [15]. Interception and impaction are important for medium and large particles ($0.1 < Dp \leq 10$ μm; Dp: diameter of particle) [14]. Above all, turbulent air flows and associated impaction are the main mechanisms resulting in the greater deposition of particles on trees than on shorter vegetation. The inertia of particles traveling in an air stream as it curves around an object, such as a leaf or stem, forces them through the boundary layer and onto the object's surface [16,17]. Knowing the mechanism of particle movement in the atmosphere is important for investigating the effect of trees on particles.

Trees are efficient scavengers of PM [10] and can serve as sinks for particulates, gases, and aerosols at the canopy level [15,18,19]. As a result of the large canopy area of leaves and the turbulent air movement created by their structure, trees effectively capture more particles than shorter vegetation [10,20]. Fowler *et al.* [6] found that woodlands in the West Midlands of England collect three times more PM10 than grasslands. Several factors determine particle capture by vegetation. These include canopy area, tree structure, particle concentration, particle size distribution, and wind speed. Tree structure disrupts the airflow inside the shelterbelt and increases impact and interception [13]. Owing to the specific aerodynamic properties of conifers, they have been shown to capture more particles than broad-leaved trees [7,15,21,22]

PM deposition on leaf surfaces (accounting for most of the PM capture) occurs by four depositing process: sedimentation caused by gravity; diffusion derived by Brownian motion; and impaction and interception resulting from turbulent flow [7,23]. Sedimentation principally affects the deposition of

large PM (10–100 μm) [7], impaction and interception affect the deposition of particles larger than 0.5 μm [24], and Brownian motion leads to the deposition of ultrafine particles (<0.1 μm).

Many studies investigated how trees capture particles on the leaf surface [2,25–27] and leaf anatomy can be a significant factor affecting particle deposition [28]. Leaf surface can absorb ultrafine PM (0.1) into leaf tissues through their stomata when Brownian diffusion is the main deposition mechanism [24,29,30]. Räsänen *et al.* [31] compared the importance of leaf surface structure, physiology, and moderate soil drought on the particle capture efficiencies of trees in a wind tunnel using NaCl particles. The study showed that conifers capture more particles when characterized by a small leaf size. Broadleaves with low leaf wettability, low stomatal density, and leaf hairiness increased particle capture. Moderate soil drought tended to increase the particle capture efficiency of Norway spruce [32] and P. sylvestris [31]. The behavior of conifer and broadleaves represents differences in structural and chemical characteristics of cuticle wax rather than wax quality [33,34]. The existing analysis shows that the influence of thermophoresis on fine particle deposition to leaf surface cannot be ignored [24].

Near-road air quality has attracted increasing attention in developed countries. The reduction of near-road air pollution by roadside barriers, such as solid noise barriers and tree stands, has been studied. Tree stands, including street trees, have been identified as an effective means for reducing air pollutants and providing aesthetic improvement in urban landscapes [35,36]. Roadside tree canopies may adjust air quality through changing air dispersion as well as by capturing air pollutants. Recent studies have found that a street tree canopy has a positive or negative effect on air quality at the pedestrian level [37,38]. The positive effect is the obstacle posed by plants to air flow, reducing air exchange especially in the vertical direction and increasing air pollutant concentrations. The negative effect is that vegetation may emit biogenic volatile organic compounds (BVOCs) and contribute to the formation of secondary organic aerosol (SOA), which is an important chemical component of airborne particulate matter [39–41].

Windbreaks or tree rows are often seen along roads and have the effect of protecting downwind surfaces from the deposition of air particles. The effects of windbreaks on airflow and turbulence have been described in several reports [42–44]. Raupach *et al.* [42] found that the fraction of particles in the oncoming flow that pass through the windbreak, or transmittance of the windbreak to particles, is related to the optical porosity. The total deposition of particles has been determined by an exchange of the particle absorption and transmission, and maximum total deposition corresponds to an optimum porosity value. Wilson [43] extended the analytical theory of Raupach *et al.* [41] for the filtering of a particulate-loaded airstream through a laterally-uniform, porous windbreak and provided the basis for a straightforward extension of an earlier formula for particle interception by a thin windbreak. Numerical simulations were also used to illustrate the ambiguity inherent in applying to a thick windbreak the pre-existing theory of particle filtering by vegetation developed by Bouvet *et al.* [44].

The main aim of this paper was to present analyses of the temporal and spatial variations of PM1, PM2.5, and PM10 mass concentration from August to October 2013, based on three months of continuous measurements inside two different road shelterbelts. We also investigated whether concentrations inside the shelterbelts differed from those over the roads, evaluated the particulate removal efficiency of the road shelterbelts at each site, and quantified the capture levels by the road shelterbelts over the three months.

2. Materials and Methods

2.1. Study Area

The study area was located in the city of Beijing in the Olympic Forest Park (40°01′N, 116°38′E), covering an area of 6.8 km^2 (Figure 1). The shelterbelts (*Populus tomentosa* and *Fraxinus chinensis* Roxb.) adjacent to the north 5th Ring Road in the northern part of the Beijing Olympic Forest Park were chosen as the main research area. The *Populus* trees were 6–10 years old and growing well. The shelterbelt was oriented from east to west. The belt plant spacing was 6 × 5 m, and the trees were arranged in rectangular crown planting. The average crown diameter was 4.5 m, average trunk diameter was 0.19 m, and average height was 23 m. *Fraxinus chinensis* Roxb. trees were 5–8 years old, and the belt had four strains causingmortality of trees, with the rest growing well. The shelterbelt orientation was largely east-west. The belt plant spacing was 7 × 8 m with a rectangular planting configuration. The average crown height was 10 m, average diameter at breast height was 17 m, and average crown width was 5.97 m. This city was selected because of its semi-humid continental monsoon climate and terrain, high summer temperatures, cold and dry winter with an average temperature of 12 °C, annual average rainfall of 640 mm, prevailing northwest winter winds, southeast winds in the summer, and average annual wind speed of 2.5 m·s^{-1}. For the monthly and daily patterns of meteorological variables conditions in the shelterbelts during the monitoring period, see Tables 1 and 2, and Figures 2 and 3.

Figure 1. Map of Beijing and the sampling site. (**A**) Olympic forest park in Beijing. Source of map: www.map.baidu.com.

Table 1. Meteorological variables inside and outside the *Populus tomentosa* shelterbelt.

Time	Inside the Forest Belt			Outside the Forest Belt		
	Wind Speed ($m \cdot s^{-1}$)	Temperature (°C)	Relative Humidity (%)	Wind Speed ($m \cdot s^{-1}$)	Temperature (°C)	Relative Humidity (%)
August 2013	0.22	28.67	58.61	0.34	29.19	57.09
September 2013	0.23	22.34	63.21	0.36	25.57	50.23
October 2013	0.32	17.22	62.43	0.42	20.13	45.57

Table 2. Meteorological variables inside and outside the *Fraxinus chinensis* Roxb. shelterbelt.

Time	Inside the Forest Belt			Outside the Forest Belt		
	Wind Speed ($m \cdot s^{-1}$)	Temperature (°C)	Relative Humidity (%)	Wind Speed ($m \cdot s^{-1}$)	Temperature (°C)	Relative Humidity (%)
August 2013	0.23	29.31	56.28	0.34	29.19	57.09
September 2013	0.25	23.59	62.38	0.36	25.57	50.23
October 2013	0.342	18.45	61.80	0.42	20.13	45.57

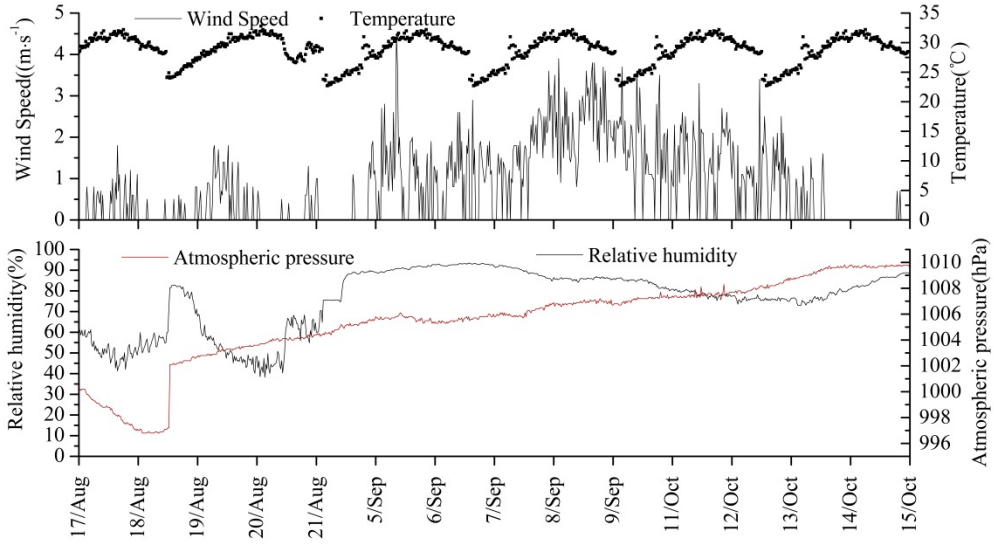

Figure 2. Meteorological variables inside the *Populus tomentosa* shelterbelt.

2.2. Collection and Measurement of Particles

Three small weather stations were installed 1.5 m above the ground inside and outside the north five ring road shelterbelts to record temperature, relative humidity, and wind speed and direction. DUSTMATE particle collector (Turnkey instruments, Northwich, UK) is a photometric sampler. It is an automatic instrument that can monitor the PM mass of PM1 (≤1 μm), PM2.5 (≤2.5 μm), PM10 (≤10 μm), and TSP. The instrument adopts the technology of scattered light to detect the concentration of dust and inhalable particles with diameter in the range of 0.4 to 20 μm. A built-in sampling pump draws in air with 10 mL/s (600 mL/min) flow, and continuous airflow containing particles passes through a laser beam in the test chamber. The light energy scattered by each particle is converted into pulses of electricity

proportional to the size of the particle. The intensity of the light pulse can determine the size of particles, using computer technology to calculate the mass of the particle. Five handheld DUSTMATE particle collectors were set up inside and outside the shelterbelts adjacent to the north five ring road at distances of 2, 20, 30, 40, and 60 m from the road. The monitoring time was from August to October 2013. The experiment was conducted for five consecutive days per month as the mean of replicate measurements. The sampling time of the day was from 7:00 to 19:00. In Figure 4 the traffic flow was higher at 08:00 and there was a slight fluctuation from 9:00 to 17:00 during the daytime; after 18:00 traffic increased and the collection was performed during this period. The DUSTMATE monitoring instruments and meteorological instruments in the forest and their layout are shown in Figure 5.

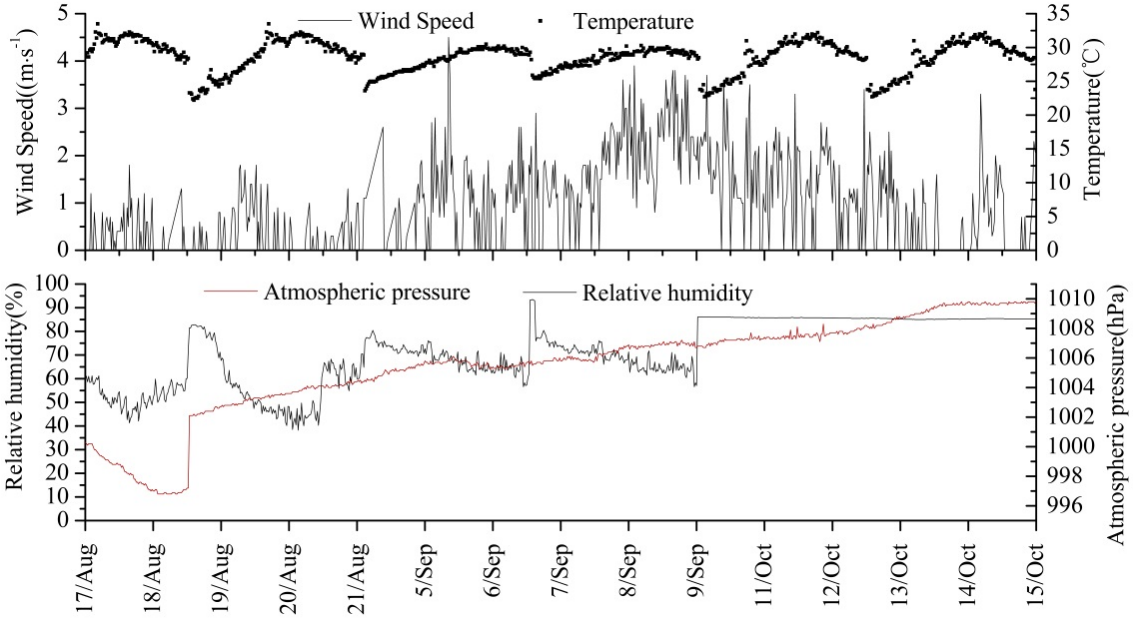

Figure 3. Meteorological variables inside the *Fraxinus chinensis* Roxb. shelterbelt.

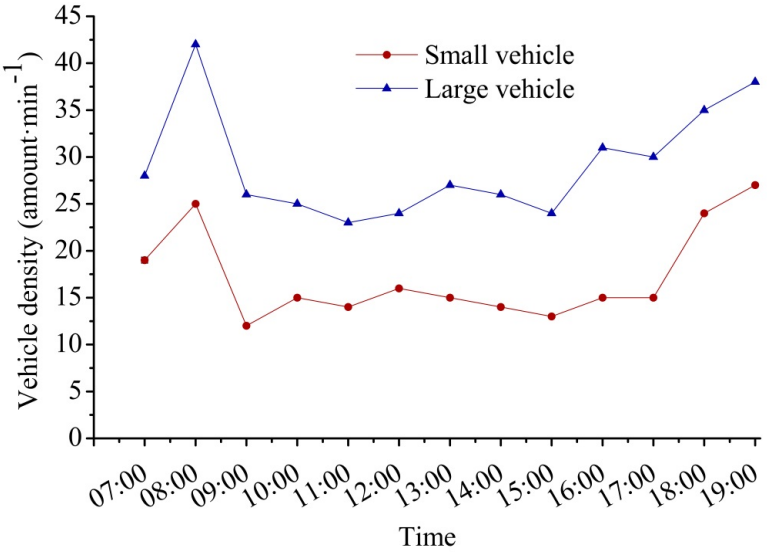

Figure 4. Traffic density during monitoring time.

The particle removal efficiency by the shelterbelts at each site was calculated by the following formula:

$$E = \frac{(C_i - C_{CK})}{C_i} \times 100\% \quad (1)$$

where C_i denotes particle concentration at the roadside in $\mu g \cdot m^{-3}$ and C_{CK} denotes particle concentration inside the road shelterbelts in $\mu g \cdot m^{-3}$.

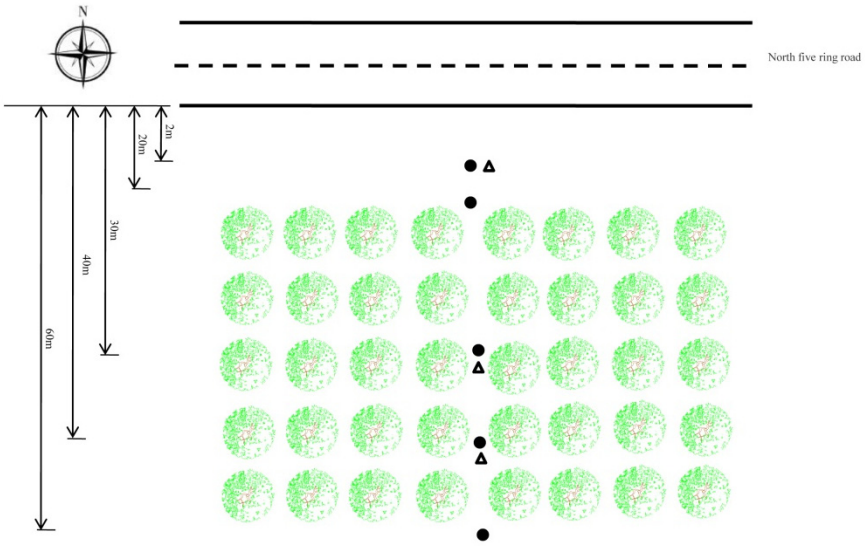

Figure 5. Particulate monitoring and meteorological instruments in wooded and open areas. Note: ● represents DUSTMATE; Δ represents the meteorological instrument. 2 m, 20 m, 30 m, 40 m, and 60 m represent the distance of DUSTMATE from the north five ring road and position in the forest belt.

2.3. Urban Forest Effects Model: Air Particulate Removed by Trees

Trees, with their large surface area of leaves and complex structure of twigs and branches, present a rough aerodynamic surface that collects particles more efficiently [13]. The important features of the study region were:

(1) two different tree species of the road shelterbelts; and
(2) shelterbelt area: the areas of the two species are the same with a length of 2000 m and a width of 60 m.

Forest removal of particulate air pollutants at a given location can be calculated from the following formula:

$$Q = F \times S \times T \quad (2)$$

where Q is the amount of a given air pollutant removed by trees in a given time (kg), F is the pollutant flux ($\mu g \cdot s^{-1} \cdot m^{-2}$), S is the total canopy cover in that area (m^2), and T is the time period(s). The pollutant flux F is calculated according to Nowak (1994a) as

$$F = V_d \times C \quad (3)$$

where V_d is the dry deposition velocity of a given air pollutant (in $m \cdot s^{-1}$) and C is the concentration of an air pollutant (in $\mu g \cdot m^{-3}$). The dry deposition process can be mentioned according to Nowak [4] as

$$V_d = \frac{1}{R_a + R_b + R_c} \quad (4)$$

where V_d is the dry deposition velocity, R_a is the aerodynamic resistance, R_b is the quasi-laminar boundary layer resistence, and R_c is the canopy resistance. R_a, R_b, and R_c were calculated according to Killus *et al.* [45] as

$$R_a = \frac{u(z)}{u_*^2} \quad (5)$$

where u(z) is the wind speed at height z ($m \cdot s^{-1}$) and u_*, the frictional velocity ($m \cdot s^{-1}$), was calculated according to Nieuwstadt [46] as

$$u_* = \frac{ku(z-d)}{\ln[(z-d)/z_0] - \psi[(z-d)/L] + \psi_m[z_0/L]} \quad (6)$$

where k is von Karman's constant (0.4), d is the displacement height (8 m), z_0 is the roughness length (0.5 m), and L is the Monin–Obukhov stability length. L has two different classification methods. One was estimated by classifying local meteorological data into stability classes using Turner classes [47] and then estimating 1/L as a function of stability class and z_0 [48]. The other method uses Pasquill's [49] stability classification scheme to classify hourly local meteorological data into stability classes.

When L < 0 (unstable condition) [50]:

$$\psi_m = 2\ln\left[\frac{(1+X)}{2}\right] + \ln\left[\frac{(1+X^2)}{2}\right] - 2\tan^{-1}(X) + 0.5 \quad (7)$$

where the dimensionless factor X is calculated according to Dyer and Bradley [51] as

$$X = \left(1 - 28\frac{z}{L}\right)^{0.25} \quad (8)$$

When L > 0 (stable condition) [50]

$$\psi_m = -17\left[1 - \exp\left(-0.29\frac{(z-d)}{L}\right)\right] \quad (9)$$

R_b was calculated according to Pederson *et al.* [52] as

$$R_b = B^{-1}u_*^{-1} \quad (10)$$

where $B^{-1} = 2(2u_*)^{-1/3}$ [45].

Hourly canopy resistance R_c values were derived from the yearly data:

$$R_c = \frac{1}{V_{g(s)}} - (R_a + R_b) \quad (11)$$

The tree canopy consistence (R_c) for the particles was derived from the literature. Nowak [4] classified canopy resistance into in-leaf season daytime, in-leaf season nighttime, and out-of-leaf season under a distribution of 90% deciduous and 10% coniferous leaf surface area. In-leaf daytime R_c was 0.78, in-leaf season nighttime Rc was 0.78, and out-of-leaf season R_c was 2.39.

V_g (m/s) is species-specific and calculated using known relationships between wind speed and V_g (using the data from Freer-Smith *et al.* [53]):

$V_{g(populus)} = 0.00125(0.5^u)$ (number of observations = 9; $p < 0.05$: $R^2 = 0.87$)

$V_{g(F.\ chinensis\ Roxb.)} = 0.00178(0.56^u)$ (number of observations = 9; $p < 0.05$: $R^2 = 0.80$),

where $V_{g(populus)}$ is the deposition velocity for *P. tomentosa*, $V_{g(F.\ chinensis\ Roxb.)}$ is the deposition velocity for *F. chinensis* Roxb., and u is wind speed.

Deposition velocities of PM2.5, PM1, and PM10 on trees were estimated from the literature and varied with wind speed [5,53–56]. Freer-Smith *et al.* [53] measured the relationship between relative deposition velocity and wind in wind tunnels. The studies showed that for *Populus*, when the wind speed is 3 $m \cdot s^{-1}$, V_d is 0.08 ± 0.01 $cm \cdot s^{-1}$; when the wind speed is 6 $m \cdot s^{-1}$, V_d is 0.2 ± 0.04 $cm \cdot s^{-1}$; and when the wind speed is 9 $m \cdot s^{-1}$, V_d is 0.36 ± 0.12 $cm \cdot s^{-1}$. For *F. chinensis* Roxb., when the wind speed is 3, 6, and 9 $m \cdot s^{-1}$, V_d is 0.25 ± 0.12 $cm \cdot s^{-1}$, 0.88 ± 0.13 $cm \cdot s^{-1}$, and 1.16 ± 0.42 $m \cdot s^{-1}$, respectively. Sun *et al.* [57] calculated a deposition velocity rate of PM2.5 in Beijing Olympic Forest Park with average day and night values of 0.9 ± 0.8 and 0.4 ± 0.5 $cm \cdot s^{-1}$. Due to this study taking place in the same experimental area as that of Sun *et al.* [57], we regard the deposition velocity of PM2.5 in this study as 0.9 ± 0.8 $cm \cdot s^{-1}$. It has been suggested that the Vg of particles of 1.0 μm diameter was between 0.4 $cm \cdot s^{-1}$ and 2.0 $cm \cdot s^{-1}$ [55,58]; here we also adopted this value. With an increase in the particle size range of 0.1–10 μm, aerosol deposition velocities are greater [58]. For PM10, the deposition velocity was assumed to be 0.64 $cm \cdot s^{-1}$ in the growing season and 0.14 $cm \cdot s^{-1}$ in the leafless season [59]; because our experiment was during the growing season, the deposition velocity of PM10 was given as 0.64 $cm \cdot s^{-1}$. The base V_d was adjusted according to the actual LAI and the in-leaf *versus* leafless season parameters. V_d changed as the LAI changed; Tallis *et al.* [15] set V_d at 0.0064 $m \cdot s^{-1}$ and assumed a single-sided LAI of 6 $m^2 \cdot m^{-2}$, 6% coniferous cover, and deposition to stems with a bark surface area of 1.7 $m^2 \cdot m^{-2}$ of land area giving a total plant area index of 7.7 $m^2 \cdot m^{-2}$. Here, we assigned a V_d of 0.9 $cm \cdot s^{-1}$ of to represent a change in LAI from 6 $m^2 \cdot m^{-2}$ between August and October, with a mean value of 4 $m^2 \cdot m^{-2}$. V_d includes an LAI parameter; the PM flux in Equation (2) is multiplied by the land area to give total flux (Q).

3. Results

3.1. Temporal Variation in Particulate Mass Concentration inside Shelterbelts

The daily variation in particle concentration measurement results inside the *Populus tomentosa* and *F. chinensis* Roxb. shelterbelts is presented in Figures 6 and 7. In the 12 h daily monitoring period, the higher value of the three particle concentrations inside the poplar forest belt appeared in August and October, and the lower value appeared in September. Particle concentration changes in the *F. chinensis* Roxb. belt showed a similar pattern to those in the *Populus* shelterbelt. Differences in PM2.5 concentration at the three monitoring times were significant. A trend of average daily concentration variation could be seen in both the poplar forest and *F. chinensis* Roxb. shelterbelt from August to October, with the particle mass concentration reaching the highest value at 08:00, and at other times, showing small fluctuations after 18:00. PM concentration continued to increase. In addition, similar results were reported by Nguyen *et al.* [60] and Wu *et al.* [61] for six urban green spaces that showed variations in air PM

concentration. They found that the PM concentrations were higher at dawn and dusk and lower at noon. Wu *et al.* [61] also reported that PM concentration was higher during the period from 19:00 to 21:00 than in the afternoon and evening. The cause of this phenomenon was rush hour traffic at approximately 08:00, and in this period of low temperature, low wind speed, and slow vertical turbulent exchange, particle diffusion was slow and PM concentration increased. After 18:00, vehicle flow increased, and a high flow of people to the Olympic Forest Park caused the PM mass concentration to rise again. In August, when the observation was interrupted by thunder showers and cloudy weather, the weather affected the particle mass concentration changes inside and outside the shelterbelts and the diurnal variation changed accordingly.

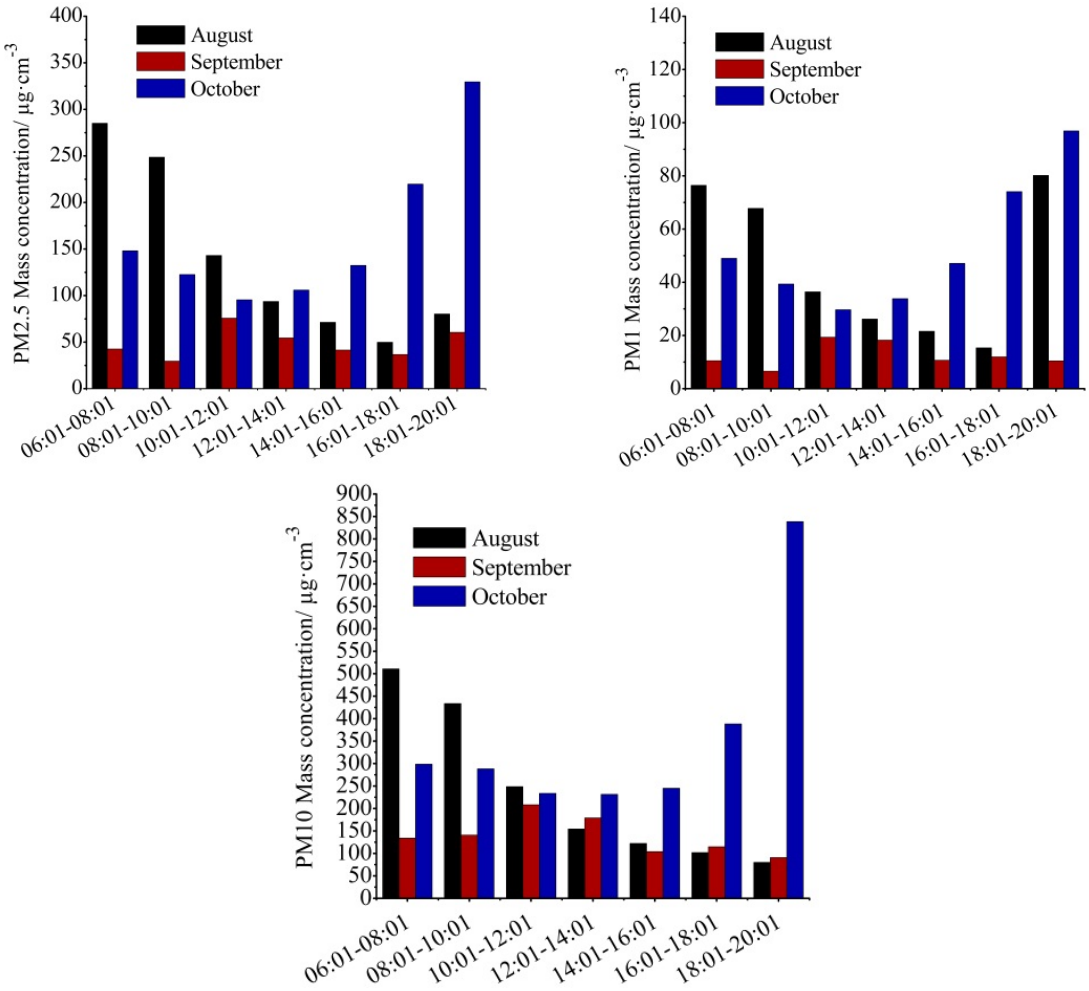

Figure 6. Daily variation in particulate mass concentration inside *Populus tomentosa* shelterbelt in different months.

The monthly average values range from 48 to 152 μg·m^{-3} for PM2.5, 13 to 49 μg·m^{-3} for PM1 and 143 to 325 μg·m^{-3} for PM10 at the *Populus* shelterbelt. At the *Fraxinus chinensis* Roxb. shelterbelt the monthly PM concentrations were somewhat lower with 32–102 μg·m^{-3} for PM2.5, 9–31 μg·m^{-3} for PM1 and 97–182 μg·m^{-3} for PM10. This may be due to the fact that *Populus* has a larger leaf surface and complex branch structure, which caused the mixture of turbulent atmospheric disturbances that can direct easy-intercept particulate matters in the air. The large tree canopy of *Populus* can also lower the air temperature through direct shading and evapotranspiration [59,62].

The average ratios between the PM fractions also split for three months are presented in Table 3. The ratios and their standard deviations are calculated from the daily means.

At the *Populus* shelterbelt site PM1 accounted for 31% of PM2.5 and for 14% of PM10 in the monthly average; for the corresponding *Fraxinus chinensis* Roxb. site the proportion of PM1 with 28% of PM2.5 and 11% of PM10 was lower. The PM1/PM2.5 ratio was very constant over both months at two shelterbelt sites. At both sites the PM10 accounted for close to 80% of TSP. The ratios of PM2.5/PM10 were 54% at the *Populus* shelter and 51% at the *Fraxinus chinensis* Roxb. shelter, which might be related to more fine particulate mobile source combustion emissions at the North five ring road, as well as climatic and emission conditions.

For Taipei, Li and Lin [63] obtained PM1/PM2.5 mass ratios as high as 0.90 in the traffic station using trichotomous samplers for sampling of the three PM fractions. Gomišček *et al.* [64] found at the urban site PM1 accounted for 82% of PM2.5 and for 57% of PM10 as an annual average; for the corresponding rural site the portion of PM1 with 84% of PM2.5 and 60% of PM10 was even higher. This relatively small difference between PM1 and PM2.5 suggests that there are almost no emission sources in this range and that fine PM is rather influenced by air mass transport. Based on two years' simultaneous one-week integrated sampling, in two downtown/residential sampling sites in Beijing, Yang *et al.* [65] reported that both PM2.5 to PM10 and PM2.5 to TSP ratios were highest in winter and lowest in spring, reflecting the fact that heating combustion sources contributed more to fine particles, while dusty weather produced more coarse particles.

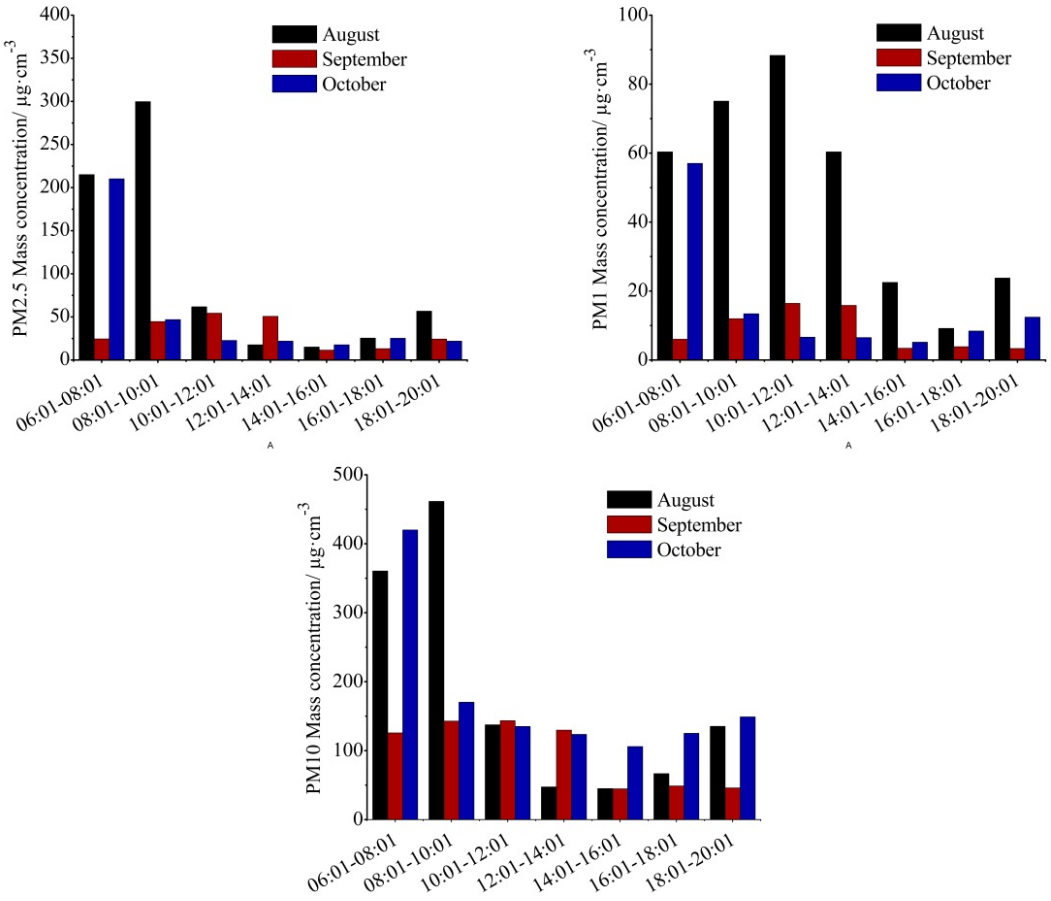

Figure 7. Daily variation in particulate mass concentration inside *Fraxinus chinensis* Roxb. shelterbelt in different months.

Table 3. Ratios (mean and standard deviation) between the various mass-fractions of PM on daily means for *Populus tomentosa* and *Fraxinus chinensis* Roxb. forest belts.

Shelterbelt/Month		PM2.5/TSP		PM1/TSP		PM10/TSP		PM1/PM10		PM2.5/PM10		PM1/PM2.5	
		Mean	**SD**	**Mean**	**SD**	**Mean**	**SD**	**Mean**	**SD**	**Mean**	**SD**	**Mean**	**SD**
Populus tomentosa	August	0.44	0.04	0.15	0.09	0.75	0.11	0.19	0.13	0.59	0.14	0.33	0.04
	September	0.27	0.01	0.07	0.13	0.82	0.11	0.09	0.09	0.55	0.04	0.27	0.01
	October	0.36	0.11	0.12	0.11	0.77	0.07	0.15	0.12	0.47	0.11	0.32	0.02
	Mean	0.36	0.05	0.11	0.11	0.78	0.10	0.14	0.11	0.54	0.10	0.31	0.02
Fraxinus chinensis Roxb.	August	0.49	0.12	0.14	0.01	0.84	0.08	0.17	0.07	0.58	0.05	0.29	0.03
	September	0.19	0.05	0.05	0.04	0.57	0.05	0.08	0.02	0.55	0.04	0.25	0.01
	October	0.25	0.07	0.07	0.02	0.94	0.13	0.08	0.02	0.39	0.03	0.30	0.04
	Mean	0.31	0.08	0.09	0.02	0.78	0.09	0.11	0.04	0.51	0.04	0.28	0.03

3.2. Particulate Mass Concentration Variation in Different Locations outside and inside Shelterbelts

Figures 8 and 9 shows the comparative results of PM mass concentration outside and inside two different shelterbelts. The PM mass concentration inside and outside shelterbelt change is significant, as the general trend of PM mass concentration inside the shelterbelt is higher than outside.

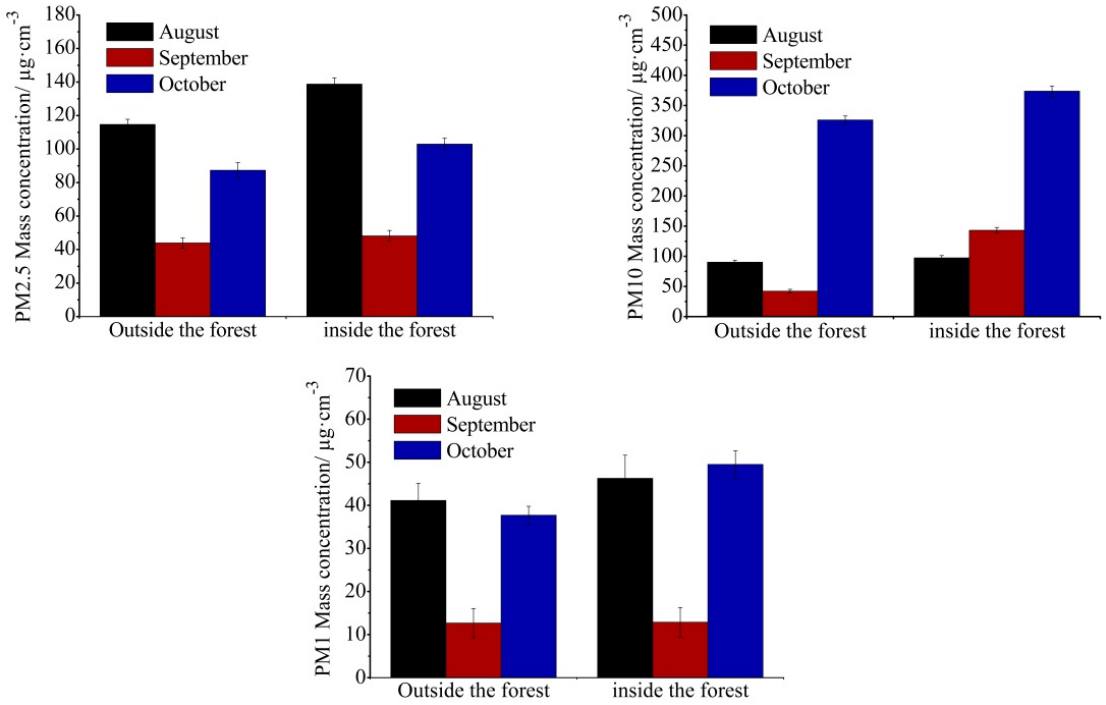

Figure 8. Comparison of PM mass concentration inside and outside the *Populus* forest belt from August to October.

The reason for this kind of phenomenon is that the spatial structure of forest belt affecting the microclimate would change the PM mass concentration inside the shelterbelt. In general, airflow through the forest belt can be divided into two parts: when lower air flow encounters the shelterbelt, owing to a blocking effect by the shelterbelt, part of the airflow moves directly through the shelterbelt gap; the friction between the airflow and the tree consumes more energy of the flow and causes the kinetic energy of the

airflow to drop, which leads to the wind speed reducing [66–69]. The reduction in wind in the shelterbelt, not conducive to the spread of PM, which is prone to settlement, eventually leads to an increase in PM mass concentration. Another part of the airflow is forced to rise above the shelterbelt.

The cause for this surprising result requires deep research. Absorption of particles by trees changed with the increasing distance from the road. Mori *et al.* [70] selected two tree species (*Picea sitchensis* Carrière and *Pinus sylvestris* L.) to test their capacity to accumulate particulate matter on the leaf surface. The study found that accumulation of PM10 decreased with distance from the road in both *P. sylvestris* and *Picea sitchenisis*, while the smaller fractions did not show any clear trends with respect to the distance from the road.

Correlation between PM mass concentration and meteorological elements inside the *Populus* and *F. chinensis* Roxb. shelterbelts are presented in Tables 4 and 5. The mass concentrations of PM are significantly and negatively correlated with temperature and wind speed, but positively correlated with air pressure as well as relative humidity.

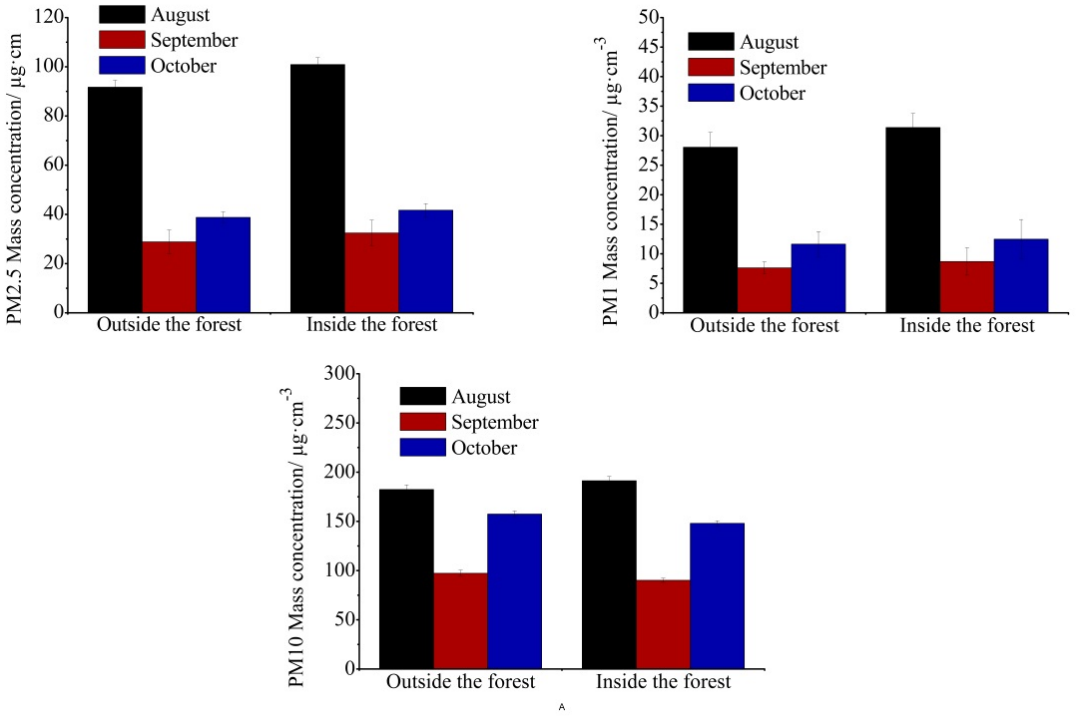

Figure 9. Comparison of PM mass concentration inside and outside the *Fraxinus chinensis* Roxb. forest belt from August to October.

Table 4. Correlation coefficients between PM2.5 mass concentration and meteorological factors inside the *Populus* shelterbelt.

Meteorological Elements	Spearman Correlation Coefficients	Two-Tailed Significance Level
Wind speed	−0.779 *	0.020
Temperature	−0.755 **	0.000
Relative humidity	0.804 **	0.000
Atmospheric pressure	0.506 **	0.000

Note: * Correlation is significant at the 0.05 level (two-tailed). Similarly hereafter; ** Correlation is significant at the 0.01 level (two-tailed).

Table 5. Correlation coefficients between PM2.5 mass concentration and meteorological factors inside the *F. chinensis Roxb.* shelterbelt.

Meteorological Elements	Spearman Correlation Coefficients	Two-Tailed Significance Level
Wind speed	−0.226 **	0.006
Temperature	−0.798 **	0.000
Relative humidity	0.657 **	0.000
Atmospheric pressure	0.090	0.276

The spatial variation in particle mass concentration among different locations inside the two shelterbelts is shown in Figures 10–12. It is clearly observed that the particle concentration reached its highest value of 40 m inside the *Populus tomentosa* shelterbelt from August to October. The optimal location for particle concentration always changes in the *F. chinensis* Roxb. shelterbelt in October. This observation leads to the question of why higher particle concentrations occur inside forest belts. The reason is probably that forest belts first intercept particles on their leaves and branches and then the particles reach the ground by dry and wet deposition.

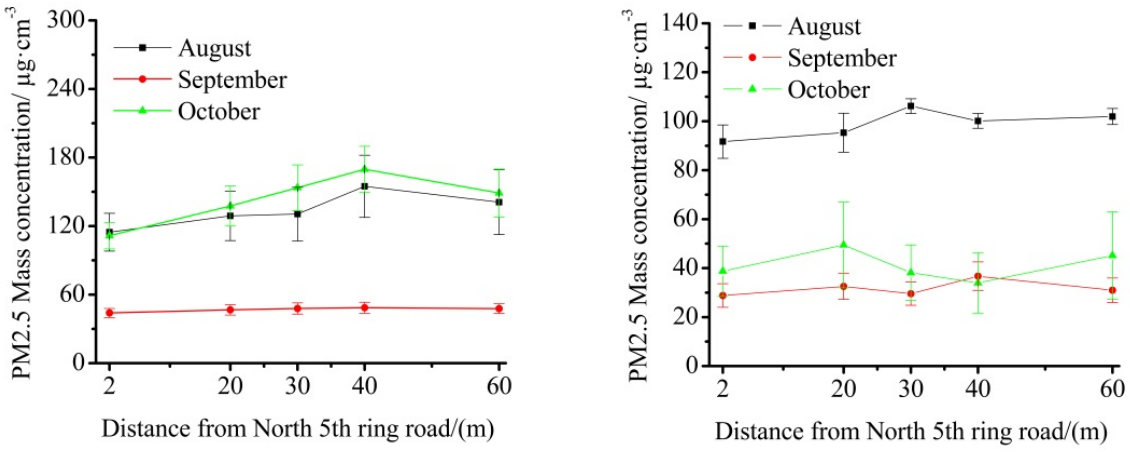

Figure 10. Comparison of PM2.5 mass concentration inside and outside the forest belt with different distances.

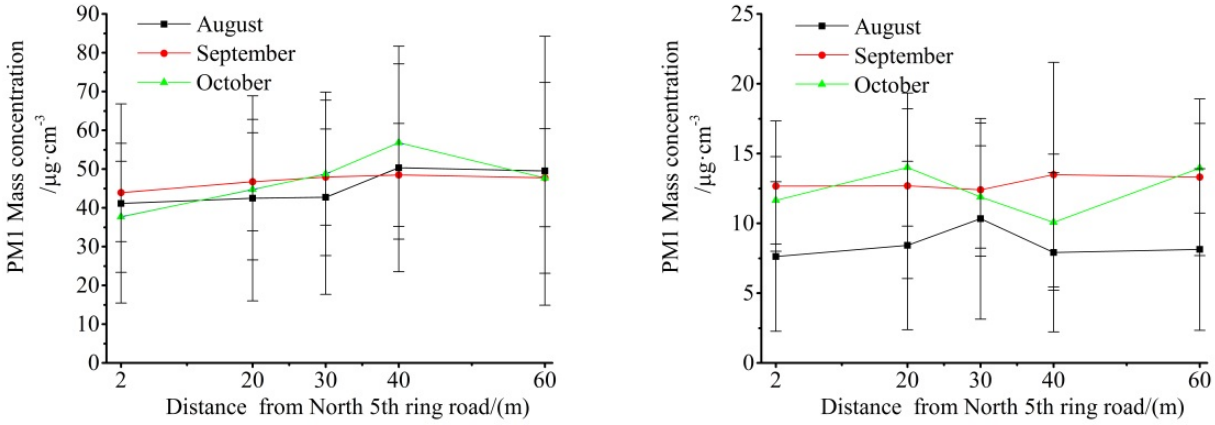

Figure 11. *Cont.*

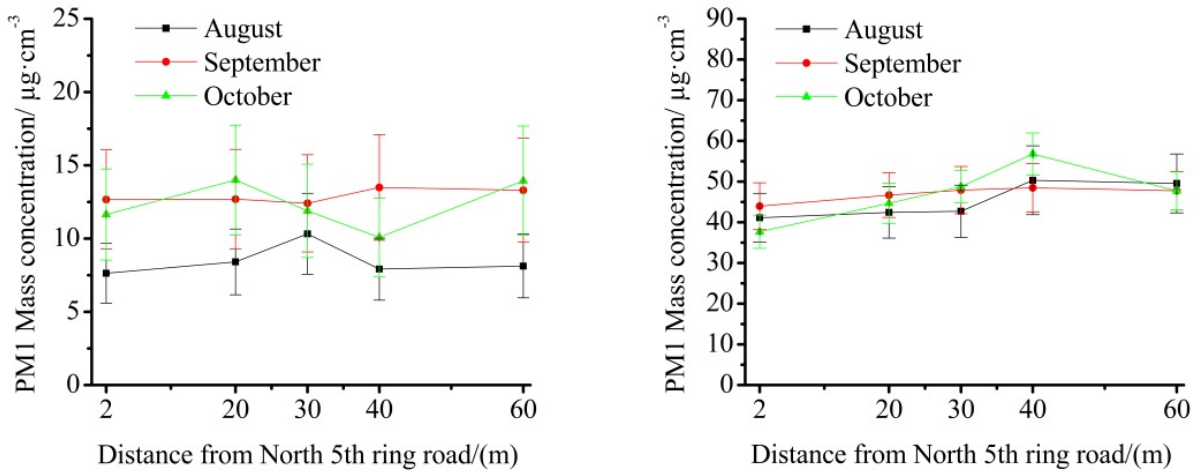

Figure 11. Comparison of PM1 mass concentration inside and outside the forest belt with different distances.

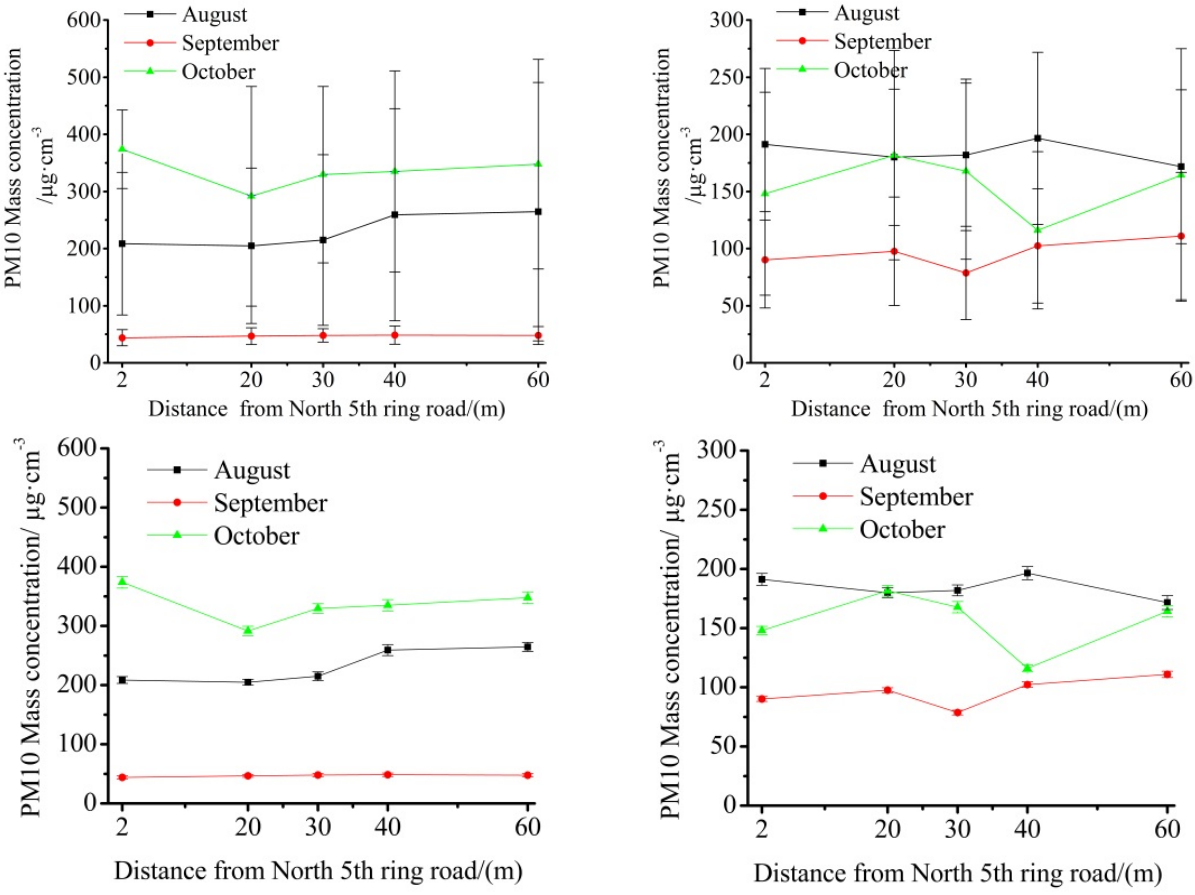

Figure 12. Comparison of PM10 mass concentration inside and outside the forest belt with different distances.

Owing to the small size of the sampling site, we used kriging interpolation to simulate the diurnal variation of PM2.5 concentration at different locations inside the two forest belts in August 2013 (Figures 13 and 14). From the contour map, we can conclude that PM2.5 concentration at different

distances reached a peak value in three time periods (morning, noon, and dusk). Therefore, a suitable forest belt width is important for particulate interception.

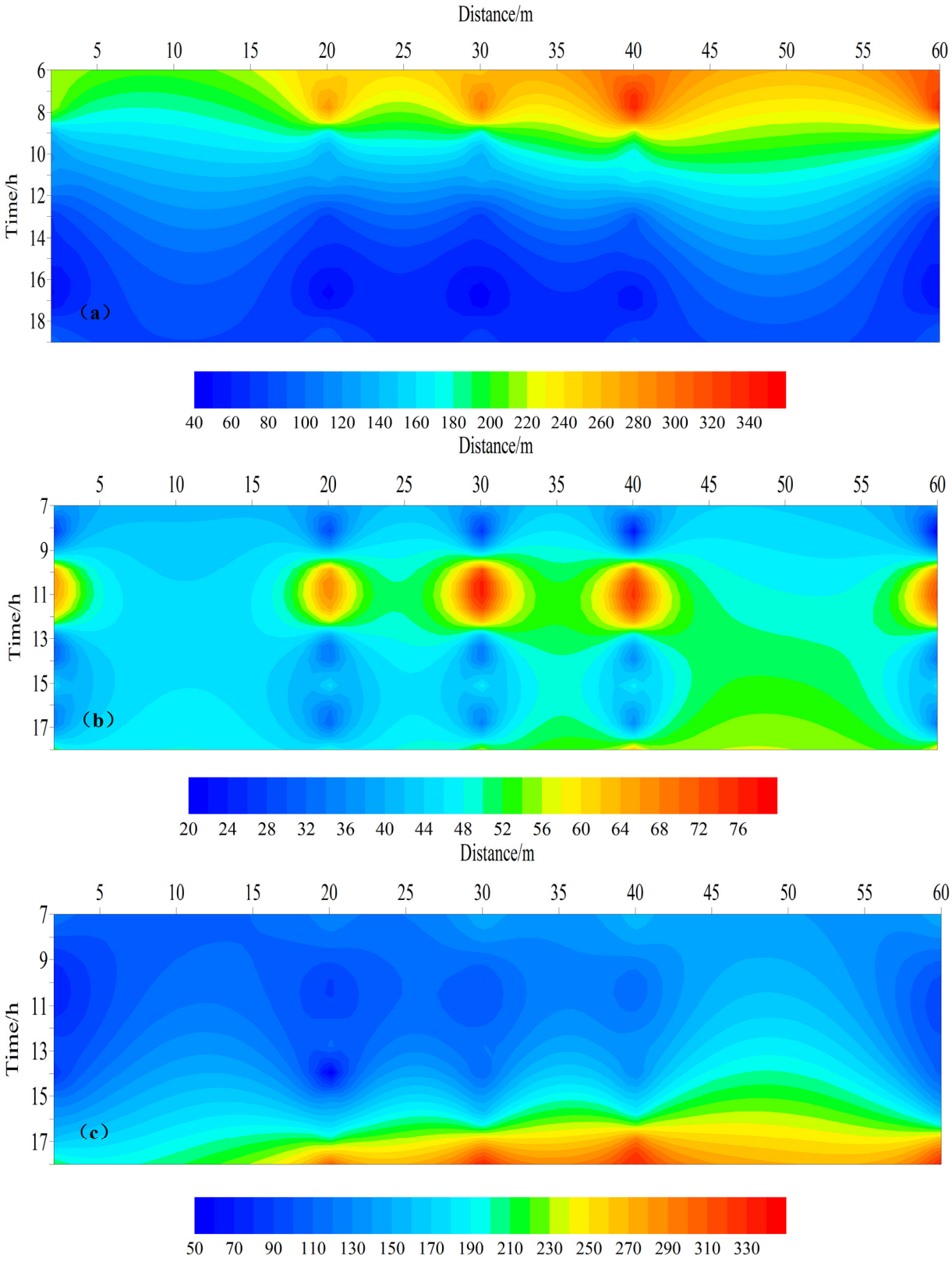

Figure 13. Diurnal variation in PM2.5 concentration at different distances inside the *Populus tomentosa* shelterbelt. Note: (**a**–**c**) are PM2.5 concentration contour plots inside *Populus tomentosa* shelterbelts in August, September, and October.

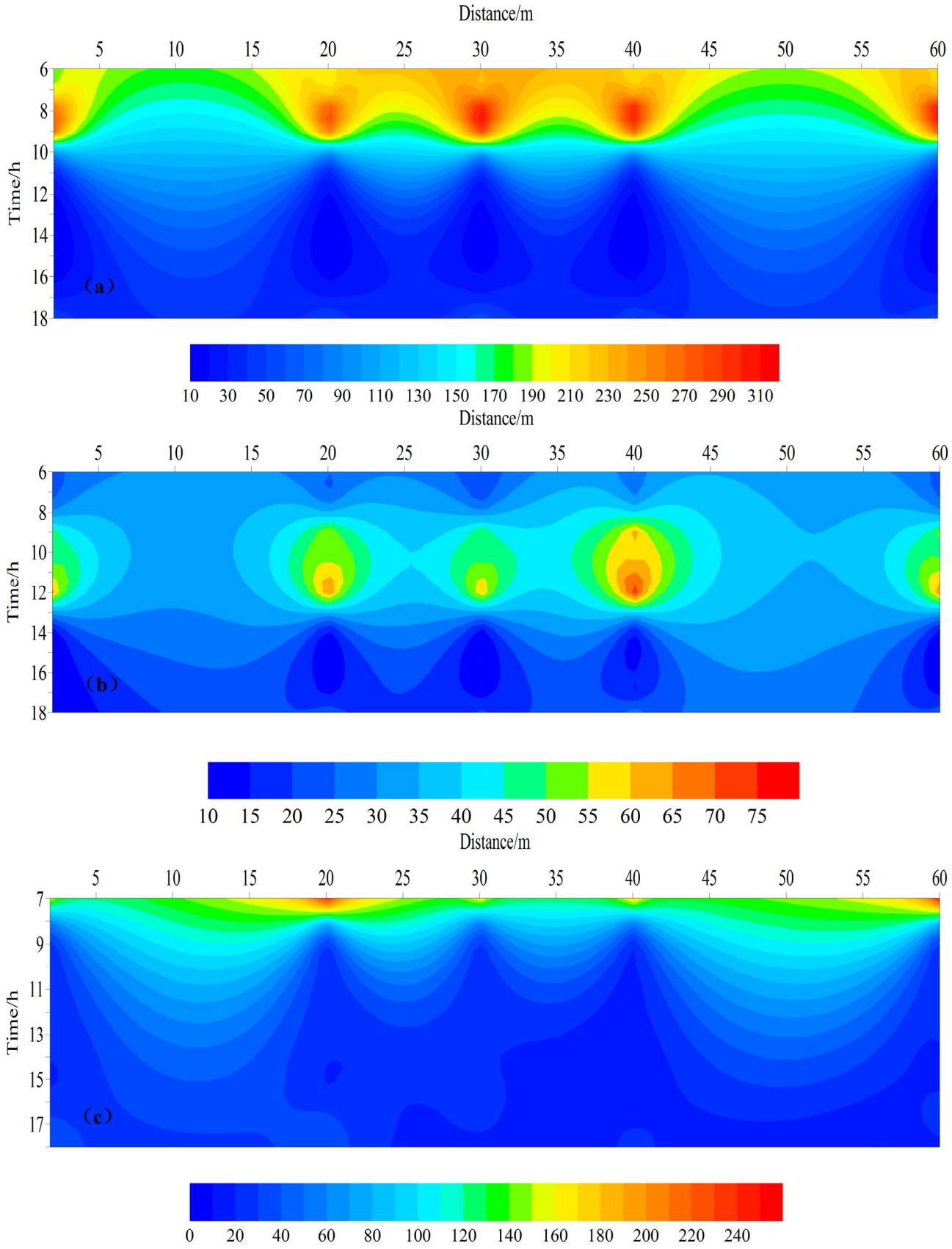

Figure 14. Diurnal variation in PM2.5 concentration at different distances inside the *Fraxinus chinensis* Roxb. shelterbelt. Note: (**a**–**c**) are PM2.5 concentration contour plots inside the *Fraxinus chinensis* Roxb. shelterbelt in August, September, and October.

3.3. Particulate Removal Efficiency

The particulate removal percentages inside the different shelterbelts in the Olympic Park are presented in Figures 15–17. Positive values denote concentrations on roadsides higher than those in the shelterbelts, and negative values denote the opposite. The higher the negative value, the higher the particulate interception efficiency. These purification effects are especially prominent within 40 m of the roadside. The PM concentration interception efficiency of the two forest belts in the three months in descending order was PM10 > PM1 > PM2.5. In both *Populus* and *F. chinensis* Roxb. shelterbelts, because of leaf senescence in October, the PM concentration declined, resulting in an increased frequency of positive values of interception efficiency.

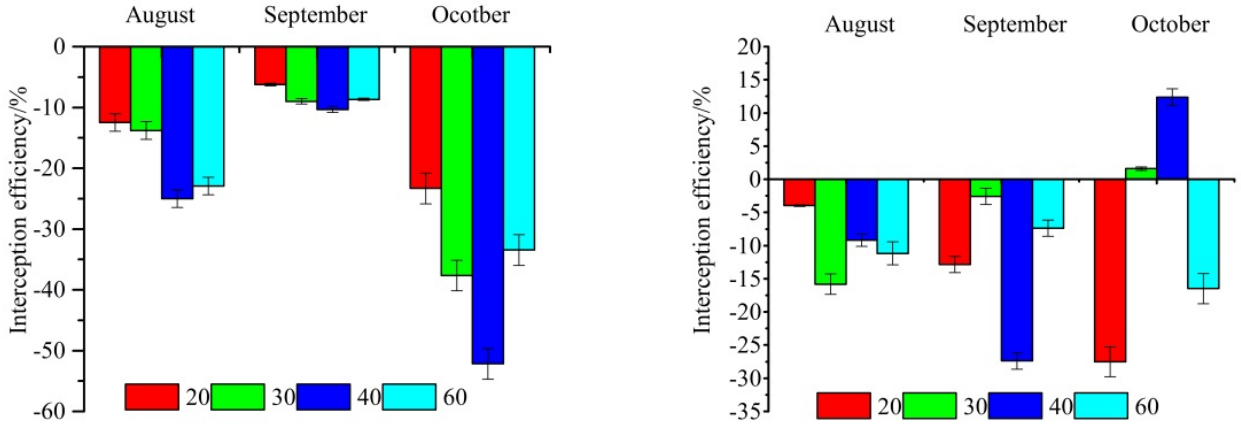

Figure 15. PM2.5 interception efficiency of the *Populus* belt (**left**) and *Fraxinus chinensis* Roxb. belt (**right**) at different locations (mean ± SD).

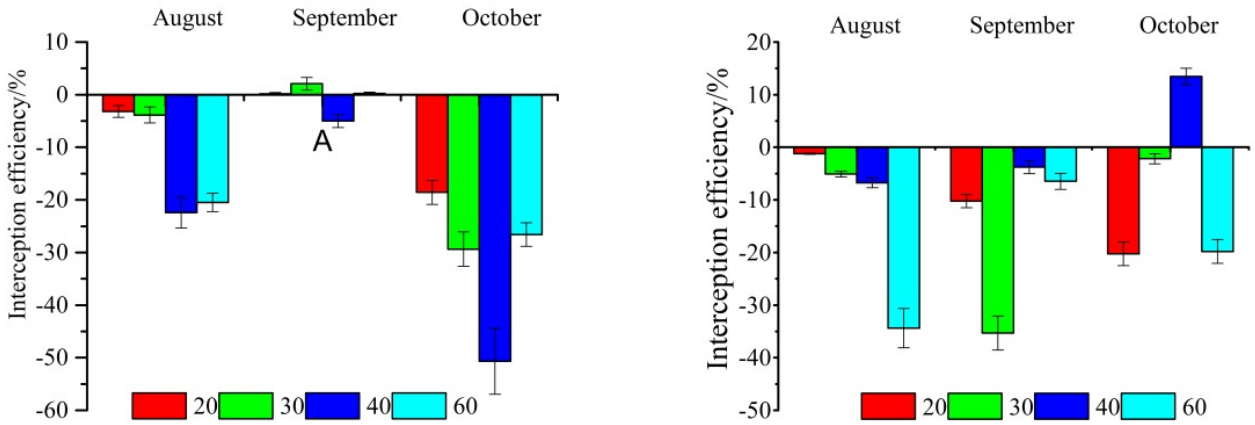

Figure 16. PM1 interception efficiency of the *Populus* belt (**left**) and *Fraxinus chinensis* Roxb. belt (**right**) at different locations (mean ± SD).

Plants retain PM on leaves and trunks when the size of leaf stomata is bigger than the particle size [31]. When the absorption retention reaches a certain amount, larger particles readily saturate stomata, resulting in low fine particle adsorption efficiency. Trees are more effective in the uptake of particles than lower vegetation, owing to the large surface area of leaves, stems, and branches and atmospheric turbulence caused by their complex internal structure [71,72]. Ultrafine particle diffusion is

accelerated by wind, so that the attenuation of fine particles is more rapid than that of large particles with distance from source [7]. Islam *et al.* [62] found the best positive correlation between TSP and crown density, negatively correlated with the shelterbelt porosity; shelterbelt porosity ranges of 20%–40% can be defined as the optimum for TSP removal. They also observed that the maximum TSP removal percentage was 65%, and the relative reduction effect was 0.4% in summer along the Khulna–Batiaghata road. This result was similar to that reported by McPherson *et al.* [73], who calculated the uptake of particulate matter by trees in Chicago. The findings of this study showed that better scavenging effects are achieved by planting appropriate vegetation as well as certain type and characteristics of trees. However, too dense configuration of the vegetation may not achieve a beneficial effect, so the construction of urban greenspace must pay attention to the structure of the greenbelt that has optimal canopy density and porosity, in addition to selecting the trees with higher capability of retaining dust.

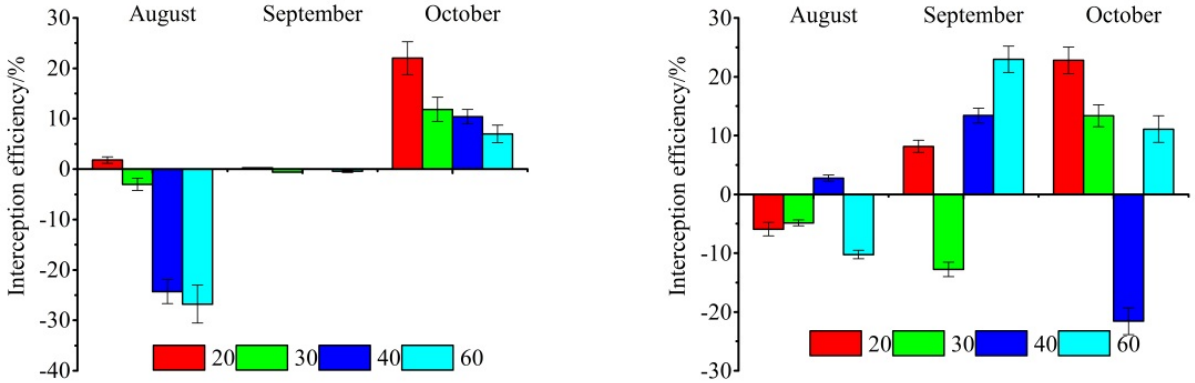

Figure 17. PM10 interception efficiency of the *Populus* belt (**left**) and *Fraxinus chinensis* Roxb. belt (**right**) at different locations (mean ± SD).

3.4. Air-Pollutant Removal

We adopted the Urban Forest Effects Model (UFORE) [4], using hourly meteorological and pollution concentration data. The results of particle interception modeling are shown in Figures 18 and 19. The total air-particulate uptake by the two tree types was 1496 and 909 kg over the three months. From the monthly average concentrations and the pollutant capture, we can conclude that the main air pollutant in Beijing in 2013 was PM10. Considering PM10 as an example, for the *Populus* shelterbelt, the total PM10 uptake by the trees was 303.25 kg during August and accounted for 52.2% of total air pollutants in the three months. Tiwary *et al.* [8], in a 10 × 10 km study area containing 75% grassland, 20% sycamore maple (*Acer pseudoplatanus* L.), and 5% Douglas fir [*Pseudotsuga menziesii* (Mirb.) Franco], calculated that PM10 removal was 90.41 t·year^{-1}, equating to 0.009 t·ha^{-1}·year^{-1} over the whole study area. This result is greater than that found in Chicago by Nowak [4], who calculated that trees within the city could reduce PM10 concentrations by 0.004 t·ha^{-1}·year^{-1}. Yang *et al.* [59], also using the UFORE model, found that trees in Beijing removed the most PM10, with the reduction amounting to 720 t, equating to 0.025 t·ha^{-1}·year^{-1} and accounting for 61% of total air pollutants. This greater value can probably be explained by the differences in climate and tree cover (16.4%) and by the higher PM10 concentrations in Beijing than in Chicago. Nowak *et al.* [9], using the UFORE model, found that the total amount of PM2.5 annually removed by trees varied from 4.7 t in Syracuse to 64.5 t in Atlanta, but in

Atlanta trees removed 423 t of PM10 [74], indicating that the removal of PM10 by trees is substantially higher than that of PM2.5. Particles deposited on the leaf surface remain there in part, with the other part resuspended in the atmosphere by wind or washed off by precipitation.

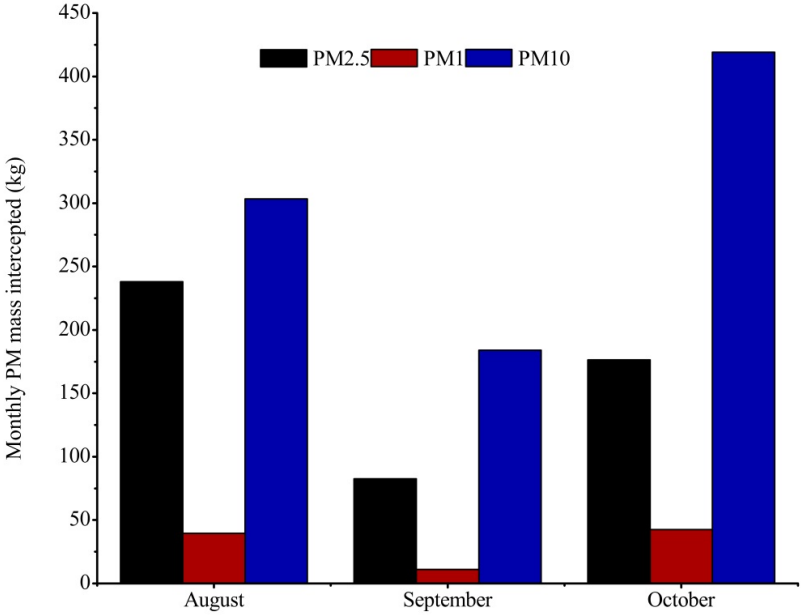

Figure 18. Monthly air-pollutant removal by the *Populus* belt.

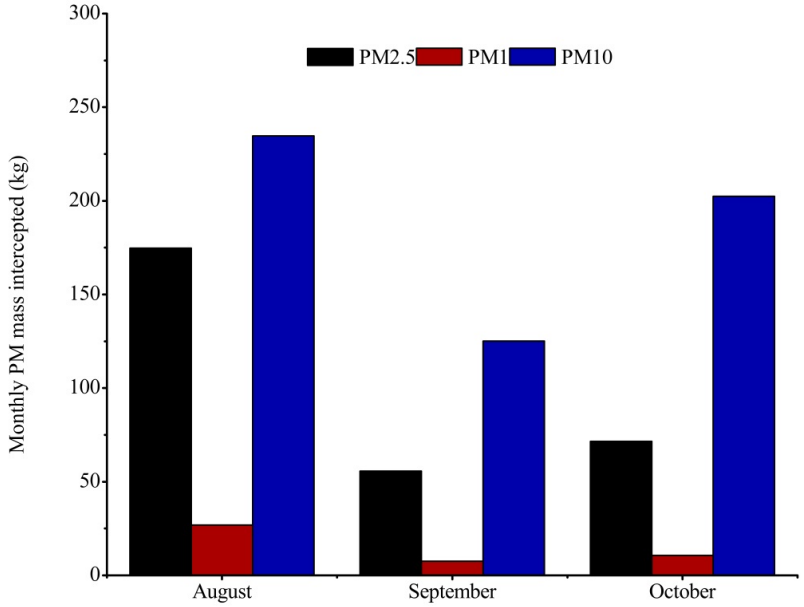

Figure 19. Monthly air-pollutant removal by the *Fraxinus chinensis* Roxb. belt.

This study assumed a canopy height of 15 m, a value likely to represent *Populus tomentosa* and *F. chinensis* Roxb. trees of 8–10 and 10–12 years of age, respectively. The ability of trees to intercept air pollutants changes with climate and growth. Leaves with large surface area or hairy, scaly, or resinous surfaces capture more particles than small or smooth leaves [4,5,13,14].

The UFORE model makes several assumptions; the results of this method are only according to the site- or regional-specific data [8]. Some data and parameters of the UFORE model for specific species

and different wind speeds are lacking, but a general method is to assign generic deposition to trees. The shortcoming of this method is that it is unlikely to represent the variation in canopy structure and microclimates within a specific site and may imprecisely estimate particle flux.

The UFORE model has many limitations and disadvantages. It takes into account only dry deposition and does not consider wet deposition, thereby likely underestimating total deposition [75]. Particles deposited on leaves, twigs, and branch surfaces of trees under gravity and impaction are not subjected to resuspension, unless variation in airflow or other disturbances occur. Ould-Dada and Baghini [76] performed a wind tunnel simulation experiment to study the resuspension of 1.85 μm MMAD silica particles in detail and found that the resuspension rate is only approximately 1%. For this reason, resuspension was not considered in this paper.

4. Discussion

Dust particle concentration reduction of road open sources has drawn increasing research attention. Measures for reduction of road particulate matter are divided into two kinds. One is source control, consisting of reducing particulate matter emissions by technology, cleaning the road, and improving the road surface to reduce particulate matter sources. The other is control to the leeward side, consisting of intercepting particulate matter in porous clapboards or windbreaks and shelterbelts. Lin *et al.* [30] and Tiwary *et al.* [77] found that a hawthorn hedge of width 2.2 m and height 1.6 m efficiently reduced particulate mass concentrations. In the present study, the width of the shelterbelts was small and used a single type of plant, so future work will focus on the structure of vegetative barriers and different numbers of tree rows.

One of the most interesting findings in our study was that the PM mass concentration inside the shelterbelt is higher than outside. This challenges the common belief that leaves and other organs of trees can capture particulate and correspondingly reduce the PM mass concentration. The unexpected observations in the current study may need to be subjected to further field research in order to explain them with a complete aerodynamic theory.

Trees can effectively remove pollutants on the rough surfaces of their leaves, twigs, and branches and by their spatial configuration [10,13,78]. However, trees are also a source of particulates, emitting pollen and biogenic volatile organic compounds that can react with nitrogen oxides and eventually form ozone [79]. This article does not consider the influence of particles derived from secondary aerosols generated by active chemical reactions under high atmospheric temperatures, a topic that awaits further research.

5. Conclusions

(1) The particle mass concentration inside the shelterbelts presented a single peak or bimodal distribution (peaks at 08:00 and 12:00) and lower mass concentrations at other times.
(2) The particle mass concentration inside the shelterbelt is higher than outside.
(3) The particle interception efficiency of the two forest belts over the three months in descending order was PM10 > PM1 > PM2.5.
(4) The two shelterbelts captured air pollutants at rates of 1496.285 and 909.075 kg/month. Based on monthly average concentrations and pollutant capture quantities, the major atmospheric pollutant in Beijing city is PM10.

This paper describes tentative research on the eco-environmental benefit of urban shelterbelts and some valuable conclusions have been achieved. It is better to plant both shrubs and large trees and to plant the shrubs in the front in a logical configuration, which has optimal efficiency on particle purification from the shelterbelt. We should notice that if the configuration of the vegetation is too dense, the air could not be dispersed in greenbelts, therefore optimal crown density and shelterbelt porosity is needed. The current size structure of the shelterbelts is not optimal for air-pollutant removal. The areas of these two shelterbelts were too limited to provide a large amount of removal. Selection of appropriate species and better management practices can enhance forest ecosystem services. The recommended indicators on particle removal efficiency and amount of particle removal will provide a technical basis for careful species selection and better management practice of urban shelterbelts in the future.

Acknowledgments

This study was supported by the research projects of forestry public welfare industry. The authors are grateful to our partners in the program for their support and comments on the manuscript. We would like to express our gratitude to the authorities at the Beijing Olympic Forest Park and Beijing Forestry University for their help and giving us access to the park to conduct experiments.

Author Contributions

Jungang Chen wrote the majority of the manuscript and performed much of the data analysis. Xinxiao Yu and Huaxin Bi supervised the research. Fenbing Sun, Xiaoxiu Lun, Yanlin Fu and Guodong Jia worked on field observation and data analysis. Zhengming Zhang, Xuhui Liu and Li Mo contributed valuable scientific ideas and discussion.

Conflicts of Interest

The authors declare no conflict of interest.

References

1. Maher, B.A.; Ahmed, I.A.; Davison, B.; Karloukovski, V.; Clarke, R. Impact of roadside tree lines on indoor concentrations of traffic-derived particulate matter. *Environ. Sci. Technol.* **2013**, *47*, 13737–13744.
2. Sæbø, A.; Popek, R.; Nawrot, B.; Gawrorńska, H.; Sæbø, A.; Gawroński, S.W. Plant species differnces in particulate matter accumulation on leaf surfaces. *Sci. Total Environ.* **2012**, *427–428*, 347–354.
3. Nizzetto, L.; Cassani, C.; di Guardo, A. Deposition of PCBs in mountains: The forest filter effect of different forest ecosystem types. *Ecotoxicol. Environ. Saf.* **2006**, *63*, 75–83.
4. Nowak, D.J. Air pollution removal by Chicago's urban forest. In *Chicago's Urban Forest Ecosystem: Results of the Chicago Urban Forest Climate Project*; McPherson, E.G., Nowak, D.J., Rowntree, R.A., Eds.; U.S. Department of Agriculture, Forest Service, Northeastern Forest Experiment Station: Radnor, PA, USA, 1994; pp. 63–82.

5. Beckett, K.P.; Freer-Smith, P.H.; Taylor, G. The capture of particulate pollution by trees at five contrasting urban sites. *Arbor J.* **2000**, *24*, 209–230.
6. Fowler, D.; Skiba, U.; Nemitz, E.; Choubedar, F.; Branford, D.; Donovan, R.; Rowland, P. Measuring aerosol and heavy metal deposition on urban woodland and grassusing inventories of 210 Pb and metal concentrations in soil. *Water Air Soil Pollut.* **2004**, *4*, 483–499.
7. Freer-Smith, P.H.; Beckett, K.P.; Taylor, G. Deposition velocities to *Sorbus aria*, *Acer campestre*, *Populus deltoides* × *trichocarpa* 'Beaupre', *Pinus nigra* and × *Cupressocyparis leylandii* for coarse, fine and ultra-fine particles in the urban environment. *Environ. Pollut.* **2005**, *133*, 157–167.
8. Tiwary, A.; Sinnett, D.; Peachy, C.; Chalabi, Z.; Vurdoulakis, S.; Fletcher, T.; Leonardi, G.; Grundy, C.; Azapagic, A.; Hutchings, T.R. An integrated tool to assess the role of new planting in PM10 capture and thehuman health benefits: A case study in London. *Environ. Pollut.* **2009**, *157*, 2645–2653.
9. Nowak, D.J.; Hirabayashi, S.; Bodine, A.; Hoehn, R.E. Modeled PM2.5 removal by trees in ten U.S. cities and associated health Effects. *Environ. Pollut.* **2013**, *178*, 395–402.
10. McDonald, A.G.; Bealey, W.J.; Fowler, D.; Dragosits, U.; Skiba, U.; Smith, R.I.; Donovan, R.G.; Brett, H.E.; Hewitt, C.N.; Nemitz, E.; *et al.* Quantifying the effect of urban tree planting on concentrations and depositions of PM10 in two UK conurbations. *Atmos. Environ.* **2007**, *41*, 8455–8467.
11. Robinson, M.S.; Zhao, M.; Zack, L.; Brindley, C.; Portz, L.; Quarterman, M.; Long, X.; Herckes, P. Characterization of PM2.5 collected during broadcast and slash-pile prescribed burns of predominately ponderosa pine forests in northern Arizona. *Atmos. Environ.* **2011**, *45*, 2087–2094.
12. Matsuda, K.; Fujimura, Y.; Hayashi, K.; Takahashi, A.; Nakaya, K. Deposition velocity of PM2.5 sulfate in the summer above a deciduous forest in central Japan. *Atmos. Environ.* **2010**, *44*, 4582–4587.
13. Beckett, K.P.; Freer, P.H.; Taylor, G. Urban woodlands: Their role in reducing the effects of particulate pollution. *Environ. Pollut.* **1998**, *99*, 347–360.
14. Beckett, K.P.; Freer-Smith, P.H.; Taylor, G. Particulate pollution capture by urban trees: Effect of species and windspeed. *Glob. Chang. Biol.* **2000**, *6*, 995–1003.
15. Tallis, M.; Taylor, G.; Sinnett, D.; Freer-smith, P. Estimating the removal of atmospheric particulate pollution by the urban tree canopy of London, under current and future environments. *Landsc. Urban Plan.* **2011**, *103*, 129–138.
16. Gallagher, M.W.; Nemitz, E.; Dorsey, J.R.; Fowler, D.; Sutton, M.A. Measurements and parameterizations of small aerosol deposition velocities to grassland, arable crops, and forest: Influence of surface roughness length on deposition. *J. Geophys. Res.* **2002**, *107*, 1–10.
17. Gregory, P.H. *The Microbiology of the Atmosphere*; Leonard Hill: New York, NY, USA, 1973.
18. Decker, E.H.; Elliott, S.; Smith, F.A.; Blake, D.R.; Rowland, F.S. Energy and material flow through the urban ecosystem. *Annu. Rev. Energy Environ.* **2000**, *25*, 685–740.
19. Urbat, M.; Lehndorff, E.; Schwark, L. Biomonitoring of air quality in the Cologne conurbation using pine needles as a passive sampler—Part I: Magnetic properties. *Atmos. Environ.* **2004**, *38*, 3781–3792.

20. Fowler, D.; Cape, T.N.; Unsworth, M.H. Deposition of atmospheric pollutants on forests. *Philos. Trans. R. Soc. Lond.* **1989**, *324*, 247–265.
21. Reinap, A.; Wiman, B.; Svenningsson, B.; Gunnarsson, S. Oak leaves as aerosol collectors: Relationship with wind velocity and particle size distribution. Experiment results and their implications. *Trees* **2009**, *23*, 1263–1274.
22. Popek, R.; Gawrorńska, H.; Sæbø, A.; Wrochna, M.; Gawroński, S.W. Particulate matter on foliage of 13 woody species: Deposition on surfaces and phytostabilisation in waxes—A 3-year study. *Int. J. Phytoremediation* **2013**, *15*, 245–256.
23. Sternberg, T.; Viles, H.; Cathersides, A.; Edwards, M. Dust particulate absorption by ivy (Hedera helix L) on historic walls in urban environments. *Sci. Total Environ.* **2010**, *409*, 162–168.
24. Hinds, W.C. *Aerosol Technology: Properties, Behavior, and Measurement of Airborne Particles*, 2nd ed.; Wiley: New York, NY, USA, 1999.
25. Yin, S.; Shen, Z.; Zhou, P.; Zou, X.; Che, S.; Wang, W. Quantifying air pollution attenuation within urban parks: An experimental approach in Shanghai, China. *Environ. Pollut.* **2011**, *159*, 2155–2163.
26. Terzaghi, E.; Wild, E.; Zacchello, G.; Cerabolini, B.E.L.; Jones, K.; Guardo, A.D. Forest Filter Effect: Role of leaves in capturing/releasing air particulate matter and its associated PAHs. *Atmos. Environ.* **2013**, *74*, 378–384.
27. Song, Y.S.; Maher, B.A.; Li, F.; Wang, X.K.; Sun, X.; Zhang, H.X. Particulate matter deposited on leaf of five evergreen species in Beijing, China: Source identification and size distribution. *Atmos. Environ.* **2015**, *105*, 53–60.
28. Rai, P.K. Environmental magnetic studies of particulates with special reference to biomagnetic monitoring using roadside plant leaves. *Atmos. Environ.* **2013**, *72*, 113–129.
29. Treshow, M.; Bell, J.N.B. *Air Pollution and Plant Life*; Wiley: New York, NY, USA, **2002**; p. 34.
30. Lin, M.; Khlystov, A. Investigation of ultrafine particle deposition to vegetation branches in a wind tunnel. *Aerosol Sci. Technol.* **2012**, *46*, 465–472.
31. Räsänen, J.V.; Holopainen, T.; Joutsensaari, J.; Ndam, C.; Pasanen, P.; Rinnan, Å.; Kivimäenpää, M. Effects of species-specific leaf characteristics and reduced water availability on fine particle capture efficiency of trees. *Environ. Pollut.* **2013**, *183*, 64–70.
32. Räsänen, J.V.; Yli-Pirilä, P.; Holopainen, T.; Joutsensaari, J.; Pasanen, P.; Kivimäenpää, M. Soil drought increases atmospheric fine particle capture efficiency of Norway spruce. *Boreal Environ. Res.* **2012**, *17*, 21–30.
33. Joureva, V.A.; Johnson, D.L.; Hassett, J.P.; Nowak, D.J. Differences in accumulation of PAHs and metals on the leaves of *Tilia* × *euchlora* and *Pyrus calleryana*. *Environ. Pollut.* **2002**, *120*, 331–338.
34. Dzierzanowski, K.; Popek, R.; Gawronska, H.; Saebø, A.; Gawronski, S.W. Deposition of particulate matter of different size fractions on leaf surfaces and in waxes of urban forest species. *Int. J. Phytoremediation* **2011**, *13*, 1037–1046.
35. Buccolieri, R.; Gromke, C.; Sabatino, S.D.; Ruck, B. Aerodynamic effects of trees on pollutant concentration in street canyons. *Sci. Total Environ.* **2009**, *407*, 5247–5256.
36. Sander, H.; Polasky, S.; Haight, R.G. The value of urban tree cover: A hedonic property price model in Ramsey and Dakota Counties, Minnesota, USA. *Ecol. Econ.* **2010**, *69*, 1646–1656.

37. Litschke, T.; Kuttler, W. On the reduction of urban particle concentration by vegetation—A review. *Meteorol. Z.* **2008**, *17*, 229–240.
38. Bealey, W.J.; McDonald, A.G.; Nemitz, R.; Donovan, R.; Dragosits, U.; Duffy, T.R.; Fowler, D. Estimating the reduction of urban PM10 concentrations by trees within an environmental information system for planners. *J. Environ. Manag.* **2007**, *85*, 44–58.
39. Zhang, H.; Ying, Q. Secondary organic aerosol formation and source apportionment in Southeast Texas. *Atmos. Environ.* **2011**, *45*, 3217–3227.
40. Liao, H.; Zhang, Y.; Chen, W.T.; Raes, F.; Seinfeld, J.H. Effect of chemistryaerosol-climate coupling on predictions of future climate and future levels of tropospheric ozone and aerosols. *J. Geophys. Res. Atmos.* **2009**, *114*, D10306.
41. Poschl, U. Atmospheric aerosols: Composition, transformation, climate and health effects. *Angew. Chem. Int. Ed.* **2005**, *44*, 7520–7540.
42. Raupach, M.R.; Woods, N.; Dorr, G.; Leys, J.F.; Cleugh, H.A. The entrapment of particles by windbreaks. *Atmos. Environ.* **2001**, *35*, 3373–3383.
43. Wilson, J.D. Deposition of particles to a thin windbreak: The effect of a gap. *Atmos. Environ.* **2005**, *39*, 5525–5531.
44. Bouvet, T.; Loubet, B.; Wilson, J.; Tuzet, A. Filtering of windborne particles by a natural windbreak. *Bound.-Layer Meteorol.* **2007**, *123*, 481–509.
45. Killus, J.P.; Meyer, J.P.; Durran, D.R.; Anderson, G.E.; Jerskey, T.N.; Reynolds, S.D.; Ames, J. *Continued Research in Mesoscale Air Pollution Simulation Modeling. Volume V: Refinements in Numerical Analysis, Transport, Chemistry, and Pollutant Removal*; EPN60013-841095a; Environmental Protection Agency: Research Triangle Park, NC, USA, 1984; p. 221.
46. Nieuwstadt, F. The Turbulent Structure of the Stable, Noctural Boundary Layer. *J. Atmos. Sci.* **1984**, *41*, 2202–2216.
47. Panofsky, H.A.; Dutton, J.A. *Atmospheric Turbulence*; Wiley: New York, NY, USA, 1984.
48. Zannetti, P. *Air Pollution Modeling*; Van Nostrand Reinhold: New York, NY, USA, 1990.
49. Pasquill, F. The estimation of the dispersion of windbourne material. *Meteorol. Mag.* **1961**, *90*, 33–49.
50. Van Ulden, A.P.; Holtslag, A.A.M. Estimation of atmospheric boundary layer parameters for diffusion application. *J. Clim. Appl. Meteorol.* **1985**, *24*, 1196–1207.
51. Dyer, A.J.; Braley, C.F. An alternative analysis of flux gradient relationships. *Boundary-layer Meteorol.* **1982**, *22*, 3–19.
52. Pederson, J.R.; Massman, W.J.; Mahrt, L.; Delany, A.; Oncley, S.; den Hartog, G.; Neumann, H.H.; Mickle, R.E.; Shaw, R.H.; Paw, U.K.T.; *et al.* California ozone deposition experiment: Methods, results, and opportunities. *Atmos. Environ.* **1995**, *29*, 3115–3132.
53. Freer-Smith, P.H.; El-Khatib, A.A.; Taylor, G. Capture of particulate pollution by trees: A comparison of species typical of semi-arid areas (*Ficus nitida* and *Eucalyptus globulus*) with European and North American species. *Water Air Soil Pollut.* **2004**, *155*, 173–187.
54. Slinn, W.G.N. Predictions for particle deposition to vegetation canopies. *Atmos. Environ.* **1982**, *16*, 1785–1794.
55. Kwiecien, M. Deposition of inorganic particulate aerosols to vegetation—A new method of estimating. *Environ. Monit. Assess.* **1997**, *46*, 191–207.

56. Pullman, M. Conifer PM2.5 Deposition and Re-Suspension in Wind and Rain Events. Master's Thesis, Cornell University, Ithaca, NY, USA, 2009; p. 51.
57. Sun, F.; Yin, Z.; Lun, X.; Zhao, Y.; Li, R.; Shi, F.; Yu, X. Deposition Velocity of PM2.5 in the Winter and Spring above Deciduous and Coniferous Forests in Beijing, China. *PLoS ONE* **2014**, *9*, 1–11.
58. White, E.J.; Turner, J. A method for estimating income of nutrients in a catch of airborne particles by a woodland canopy. *J. Appl. Ecol.* **1970**, *7*, 441–461.
59. Yang, J.; McBride, J.; Zhou, J.; Sun, Z. The urban forest in Beijing and its role in air pollution reduction. *Urban For. Urban Green.* **2005**, *3*, 65–78.
60. Nguyen, T.; Yu, X.; Zhang, Z.; Liu, M.; Liu, X. Relationship between types of urban forest and PM2.5 capture at three growth stages of leaves. *J. Environ. Sci.* **2015**, *27*, 33–41.
61. Wu, Z.P.; Wang, C.; Xu, J.N.; Hu, L.X. Air-borne anions and particulate matter in six urban green spaces during the summer. *J. Tsinghua Univ. Sci. Technol.* **2007**, *47*, 2152–2157.
62. Islam, M.N.; Rahman, K.S.; Bahar, M.M.; Habib, M.A.; Ando, K.; Hattori, N. Pollution attenuation by roadside greenbelt in and around urban areas. *Urban For. Urban Green.* **2012**, *11*, 460–464.
63. Li, C.-S.; Lin, C.-H. PM1/PM2.5/PM10 characteristics in the urban atmosphere of Taipei. *Aerosol Sci. Technol.* **2002**, *36*, 469–473.
64. Gomišček, B.; Hauck, H.; Stopper, S.; Preining, O. Spatial and temporal variations of PM1, PM2.5, PM10 andparticle number concentration during the AUPHEP—Project. *Atmos. Environ.* **2004**, *38*, 3917–3934.
65. Yang, F.M.; He, K.B.; Ma, Y.L.; Zhang, Q.; Yu, X.C. Variation characteristics of PM2.5 concentration and its relationship with PM10 and TSP in Beijing. *China Environ. Sci.* **2002**, *22*, 506–511.
66. Zhu, T.Z.; Guan, D.X.; Zhou, G.S.; Jin, C.J. Review of ecological effect research of farmland sheltbelts. In *Theory of Eco-engineering of Farmland Protective Plantation*; Chinese Forestry Press: Beijing, China, 2001; pp. 91–92.
67. Telenta, M.; Duhovnik, J.; Kosel, F.; Šajn, V. Numerical and experimental study of the flow through a geometrically accurate porous wind barrier model. *J. Wind Eng. Ind. Aerodyn.* **2014**, *124*, 99–108.
68. Plate, E.J. The aerodynamics of shelterbelts. *Agric. Meteorol.* **1971**, *8*, 203–211.
69. Huang, L.M.; Chan, H.C.; Lee, J.-T. A numerical study on flow around nonuniform porous fences. *J. Appl. Math.* **2012**, *12*, 1–12.
70. Mori, J.; Hanslin, H.M.; Burchi, G.; Sæbø, A. Particulate matter and element accumulation on coniferous trees at different distances from a highway. *Urban For. Urban Greening* **2015**, *14*, 170–177.
71. Lovett, G.M. Atmospheric deposition of nutrients and pollutants in North America: An ecological perspective. *Ecol. Appl.* **1994**, *4*, 629–650.
72. Powe, N.A.; Willis, K.G. Mortality and morbidity benefits of air pollution (SO_2 and PM10) absorption attributable to woodland in Britain. *J. Environ. Manag.* **2004**, *70*, 119–128.
73. McPherson, E.G.; Nowak, D.J.; Rowntree, R.E. *Chicago's Urban Forest Ecosystem: Results of the Chicago Urban Forest Climate Project*; USDA General Training Report NE-186; Northeastern Forest Experiment Station: Radnor, PA, USA, 1994.

74. Nowak, D.J.; Crane, D.E.; Stevens, J.C. Air pollution removal by urban trees and shrubs in the United States. *Urban For. Urban Greening* **2006**, *4*, 115–123.
75. Graustein, W.C.; Turekian, K.K. The effects of forests and topography on the deposition of sub-micrometer aerosols measured by lead-210 and cesium-137 in soils. *Agric. For. Meteorol.* **1989**, *47*, 199–220.
76. Ould-Dada, Z.; Baghini, N.M. Resuspension of small particles from tree surfaces. *Atmos. Environ.* **2001**, *35*, 3799–3809.
77. Tiwary, A.; Reff, A.; Colls, J.J. Collection of ambient particulate matter by porous vegetation barriers: Sampling and characterization methods. *J. Aerosol Sci.* **2008**, *39*, 40–47.
78. Fowler, D. Pollutant deposition and uptake by vegetation. In *Air Pollution and Plant Life*; Bell, J.N.B., Treshow, M., Eds.; John Wiley and Sons, Ltd.: New York, NY, USA, **2002**; pp. 43–67.
79. Abelsohn, A.; Stieb, D.; Sanborn, M.D.; Weir, E. Indentifying and managing adverse environmental health effects 2: Outdoor air pollution. *Can. Med. Assoc. J.* **2002**, *166*, 1161–1167.

© 2015 by the authors; licensee MDPI, Basel, Switzerland. This article is an open access article distributed under the terms and conditions of the Creative Commons Attribution license (http://creativecommons.org/licenses/by/4.0/).